Accepted Manuscript

A "reactive" turn-on fluorescence probe for hypochlorous acid and its bioimaging application

Yunling Gao, Yong Pan, Yu Chi, Yuanyuan He, Haiyan Chen, Victor N. Nemykin

PII:	S1386-1425(18)30754-6
DOI:	doi:10.1016/j.saa.2018.07.090
Reference:	SAA 16359
To appear in:	*Spectrochimica Acta Part A: Molecular and Biomolecular Spectroscopy*
Received date:	14 May 2018
Revised date:	23 July 2018
Accepted date:	30 July 2018

Please cite this article as: Yunling Gao, Yong Pan, Yu Chi, Yuanyuan He, Haiyan Chen, Victor N. Nemykin , A "reactive" turn-on fluorescence probe for hypochlorous acid and its bioimaging application. Saa (2018), doi:10.1016/j.saa.2018.07.090

A "reactive" turn-on fluorescence probe for hypochlorous acid and its bioimaging application

Yunling Gao[a,c*], Yong Pan[a], Yu Chi[a], Yuanyuan He[b], Haiyan Chen[b**], Victor N. Nemykin[c***]

[a] *State Key Laboratory Breeding Base of Green Chemistry Synthesis Technology, College of Chemical Engineering, Zhejiang University of Technology, Hangzhou 310032, China.*

[b] *Department of Biomedical Engineering, School of Engineering, China Pharmaceutical University, Nanjing 210009, China.*

[c] *Department of Chemistry, University of Manitoba, Winnipeg, MB R3T 2N2, Canada*

*Corresponding author: Tel: +86-571-88320951; Email address: gaoyl@zjut.edu.cn

**Corresponding author: Tel: +86-25-83271080; Email address: chenhaiyan@cpu.edu.cn

**Corresponding author: Tel: +1-204-474-9265; Email address: Victor.Nemykin@umanitoba.ca

Abstract

An **aza-BODIPY-CNOH** probe attached aldoxime group demonstrated the specific detection for hypochlorous acid by the turn-on red emission signal. NMR, IR, and HRMS experiments confirmed that the fluorescence originated from the oxidation degradation of the non-fluorescence, aldoxime-based **aza-BODIPY-CNOH** probe into the red-fluorescence, nitrile oxide-based aza-BODIPY compound **aza-BODIPY-CNO**. The **aza-BODIPY-CNOH** probe showed good biocompatibility and was low toxic to living cells as shown from MTT experiments. Living RAW264.7 cells imaging indicated the **aza-BODIPY-CNOH** probe had good permeability and either exogenous or endogenous HClO caused the intracellular bright-red fluorescence, showing its potential hypochlorous acid-specific sensing ability in biological systems.

Keywords: aza-BODIPY, aldoxime, turn-on probe, red-emission

1. Introduction

Fluorescent dyes are widely applied in chemosensors [1-4], optical data storage[5, 6], photodynamic therapy[7-9], and biological imaging[10-13]. Visible to near-infrared fluorescent dyes have attracted wide interests in biological sensing filed, and well developed as fluorescence probes or sensors due to their high sensitivity and specify, real-time vitalization, much deeper light penetration in the tissue and lower the interference of auto-fluorescence than ultraviolet fluorescence dyes. Among these fluorescent dyes, aza-BODIPYs [14-17] are excellent candidates, as they have good photo-stability, high molar absorption coefficients, narrow absorption/emission band and good fluorescence quantum yield. In addition, their electric structures and optical properties are easy to tailor, therefore various aza-BODIPYs were proposed as optical sensors[18-20], photodynamic therapy agents[21-25], photoredox catalysts[26-28], solar energy materials[29-31] and the super molecular building blocks[32].

Hypochlorous acid (HClO) is a significant reactive oxygen species (ROS) in living organisms mainly produced from the myeloperoxidase-catalyzed (MPO) reaction of hydrogen peroxide and chloride ion[33, 34]. HClO plays a critical role to defense invading bacterial in living organisms. However high concentration level of HClO would damage the tissue and cause various diseases, such as arthritis[35, 36], kidney disease[37, 38], cardiovascular disease[39], and even cancer[40]. Therefore, the real-time monitoring HClO level in living organisms is very important and highly demanded.

Fluorescence probes with the capability of the real-time visual detection of HClO, have been rapidly developed in recent years [41, 42]. Various recognition groups sensitive to HClO, such as chalcogenide[43, 44], *p*-methoxyphenol[45], hydroxylamine[46, 47] and acylhydrazine[48, 49], were used in design and synthesis of the HClO-specific probes. Among them, an aldoxime group[50, 51] frequently is employed to successfully design turn-on HClO probes where the HClO oxidation of the aldoxime group removes its

rotation and isomerization effects to light up the fluorescence. In this work, an aldoxime-based aza-BODIPY core probe (**aza-BODIPY-CNOH**) was synthesized. The turn-on probe showed the excellent selectivity to HClO over multiple oxidants and physiologically relevant ions. The sensing mechanism was well established using NMR and HRMS. In addition, the probe was applied in living cells to explore exogenous and endogenous HClO detection.

2. Results and discussion

2.1 Synthesis and characterization of the aza-BODIPY-CNOH probe

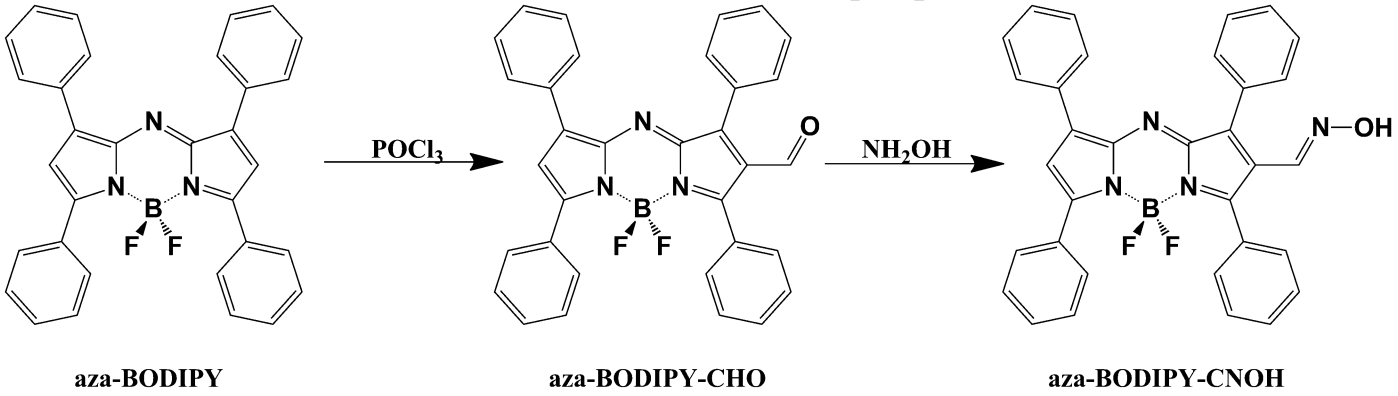

Scheme 1. Synthesis of the **aza-BODIPY-CNOH** probe.

The **aza-BODIPY-CNOH** probe was easily prepared from aza-BODIPY aldehyde reacted with hydroxylamine sulfate in pyridine at 60 °C (Scheme 1), and characterized using ^{1}H NMR, ^{13}C NMR, IR, and HRMS (Figs. S1-3). ^{1}H NMR spectrum (Fig. S1) shows the aldehyde peak at 9.79 ppm has disappeared and the HRMS confirmed the formation of the probe **aza-BODIPY-CNOH** with the m/z at 559.1927 ($[M-H]^-$) (Fig. S3).

2.2 Spectroscopic properties of the aza-BODIPY-CNOH probe

The **aza-BODIPY-CNOH** probe is almost non-fluorescence in the test solution (HEPES-acetonitrile, v/v = 1:1, pH = 7.2) with the quantum yield at 0.0012 (Fig. 1a). When 10 μM **aza-BODIPY-CNOH** was subjected to the 300 μM of sodium hypochlorite solution (pH = 7.2), an increase in the red fluorescence was observed.

The fluorescent intensity increase was 7.7 times compared to that of the probe alone, which suggested that the **aza-BODIPY-CNOH** probe might be oxidized since the aldoxime H-C=N-OH group probably tends to isomerize and rotate to quench fluorescence by a non-radiative deactivation[52, 53]. In addition, the maximum emission wavelength was red-shifted to 667 nm from 660 nm (Φ_{FL} =0.0094). Uv-vis spectrum of the **aza-BODIPY-CNOH** probe showed the decrease of absorbance at 636 nm and slight blue-shift to 631 nm with the addition of 300 μM of sodium hypochlorite solution (Fig. 1b).

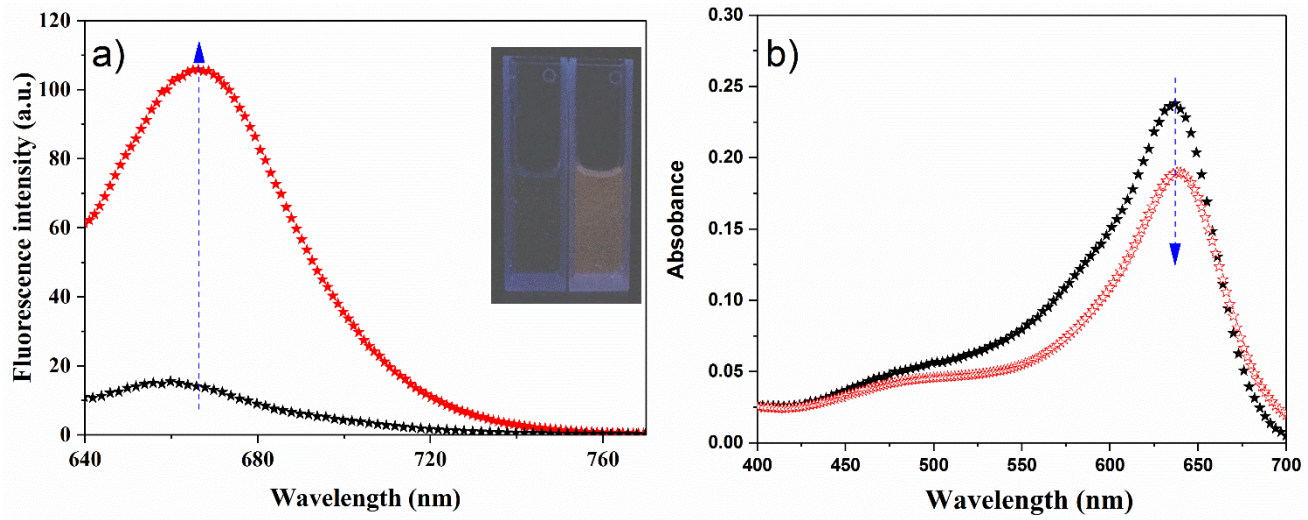

Fig. 1. Fluorescence (a) and UV-vis spectra (b) of the **aza-BODIPY-CNOH** probe (10 μM) in the absence and presence of sodium hypochlorite (300 μM) in HEPES/CH_3CN (1:1, pH = 7.2) solution. Red stars: sodium hypochlorite plus the probe; black stars: the probe alone.

The fluorescent titrations of the **aza-BODIPY-CNOH** probe with sodium hypochlorite solution were then carried out shown in Fig. 2. The gradual increase in fluorescent intensity was observed with the addition of sodium hypochlorite up to 150 μM (Fig. 2a). Meanwhile, the **aza-BODIPY-CNOH** probe has undergone a distinct emission change from the non-fluorescence to red. The fluorescent intensity demonstrated the good linearity with the concentration of sodium hypochlorite in the range of 0 to 120 μM based on the linear equation $y = 2.92x + 13.66$ with a linear coefficient of 0.997. The limit of detection was calculated as 2.33 μM (Fig. 2b).

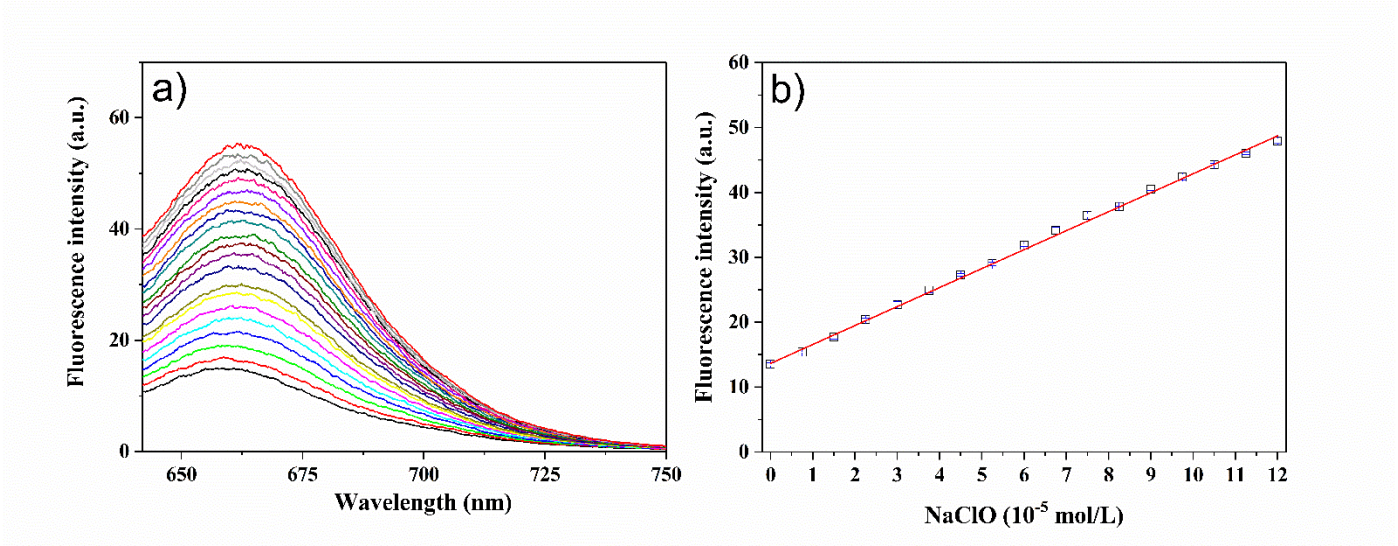

Fig. 2. a) Fluorescent changes of the **aza-BODIPY-CNOH** probe with the addition of different concentrations of sodium hypochlorite (0-150 μM) in HEPES/CH_3CN (1:1, pH = 7.2) solution. **b)** The linear relationship of the fluorescence intensity and the concentration of sodium hypochlorite at 667 nm.

2.3 Selectivity of the aza-BODIPY-CNOH probe

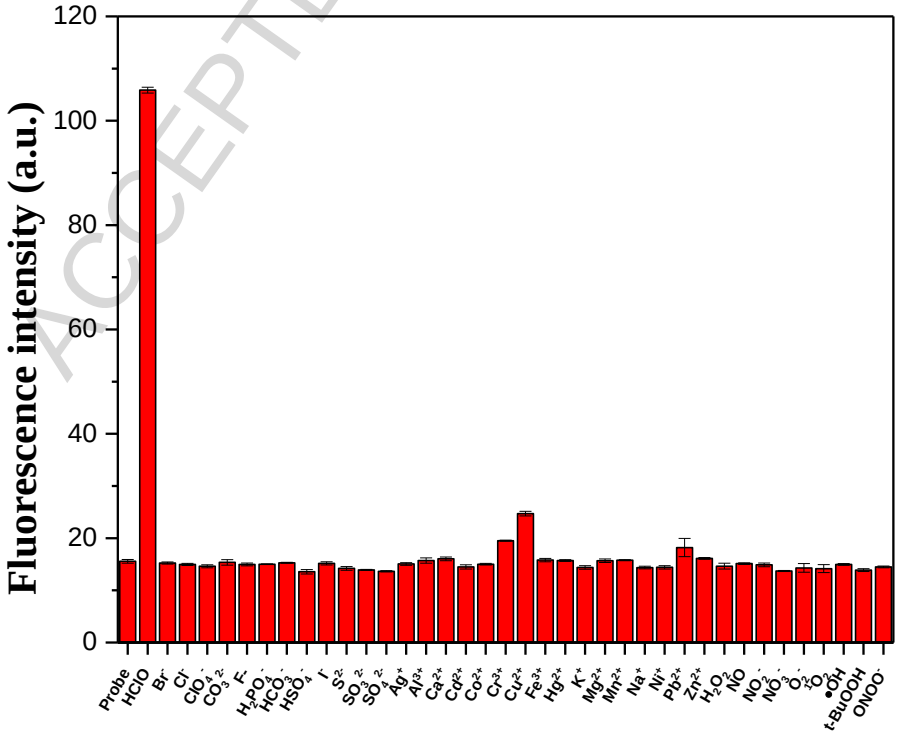

Fig. 3. Fluorescence intensity changes of the **aza-BODIPY-CNOH** probe (10 μM) with the addition of individual ions (300 μM).

In order to determine the selectivity of the **aza-BODIPY-CNOH** probe, other ROS/RNS species including H_2O_2, NO, NO_2^-, NO_3^-, O_2^-, $^1O_2$, ·OH, $ONOO^-$ and t-BuOOH were added individually to the 10 μM probe solution. As showed in Fig. 3, these ROS/RNS species caused no appreciable fluorescence changes. Similarly, common anions, like F^-, Cl^-, Br^-, I^-, HCO_3^-, CO_3^{2-}, HSO_4^{2-}, $H_2PO_4^-$, ClO_4^-, S^{2-}, SO_3^{2-} and SO_4^{2-}, did not affect the fluorescence of the probe. Meanwhile, common metal cations were also explored (Al^{3+}, Ca^{2+}, Zn^{2+}, Pb^{2+}, Cr^{3+}, Fe^{3+}, Cu^{2+}, Hg^{2+}, K^+, Mn^{2+}, Mg^{2+}, Na^+, Ni^+ and Ag^+) and showed negligible effect on the probe. Hereby, the **aza-BODIPY-CNOH** probe showed the specific sensing ability for hypochlorous acid.

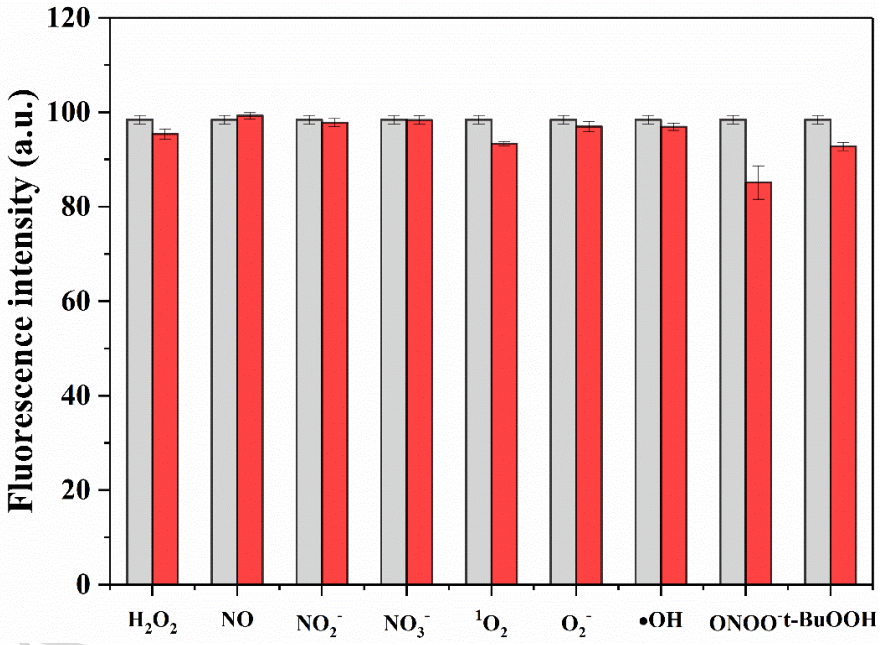

Fig. 4. Effects of various interfering ROS/RNS (300 μM) species on the fluorescence intensity of the **aza-BODIPY-CNOH** probe at 667 nm. Grey bars: aza-BODIPY-CNOH plus sodium hypochlorite; Red bars: aza-BODIPY-CNOH plus sodium hypochlorite followed by adding other ROS/RNS.

Next, the competition experiments were performed to test whether the **aza-BODIPY-CNOH** probe can sense hypochlorous acid efficiently and the results were shown in Fig. 4 and Fig. S4. As expected, Figure 4

shows that the ROS/RNS species have not obvious effect on the fluorescence of the **aza-BODIPY-CNOH** probe in sensing hypochlorous acid except slight decrease in fluorescent intensity for $ONOO^-$. Meanwhile, the addition of hypochlorous acid caused distinct fluorescence increase after the **aza-BODIPY-CNOH** probe was treated with different interfering ROS/RNS species (Fig. S4). Therefore, the **aza-BODIPY-CNOH** probe demonstrated the good anti-interference ability to other ROS/RNS species and could be an excellent turn-on fluorescence probe for detection of hypochlorous acid.

2.4 pH effect on the aza-BODIPY-CNOH probe

Aldoxime group in the structure of **aza-BODIPY-CNOH** might undergo protonation or deprotonation as a function of pH values, therefore the relative fluorescence of the probe was studied in the presence and absence of sodium hypochlorite solution. The pH titrations were performed with the 10 μM probe **aza-BODIPY-CNOH** in the absence or presence of 50 μM sodium hypochlorite solution (Fig. S5). The **aza-BODIPY-CNOH** probe kept the negligible changes of the weak fluorescence in the range of pH 2 to 13, while in the presence of sodium hypochlorite, the fluorescence intensities were increased over the whole test pH range, indicating the **aza-BODIPY-CNOH** probe has potential to sensing both HClO and ClO^-. Although the fluorescence intensities have got the extremely significant increase in the alkali region (pH 8 to 12) where the sensing species are probably dominated by hypochlorite (pKa_{HClO} = 7.5[54]), the experiments were still set up at pH = 7.2 because the physiological pH values are preferred at neutral in biological system[55] where HClO can be detected by the probe using the fluorescence. Another reason to use pH 7.2 in all experiments was the probe may be less stable in more alkali pH, as was seen the decrease fluorescence at pH 13 in Fig. S5.

2.5 Sensing mechanism

NMR and HRMS experiments were carried out to explore the mechanism of the turn-on fluorescence of the **aza-BODIPY-CNOH** probe by HClO (Fig. 5). The excess sodium hypochlorite was added to the probe solution in chloroform monitored by TLC to monitor an appearance of a new compound with the red fluorescence. The product was purified using flash column chromatography and characterized by NMR and HRMS (Fig. 5).

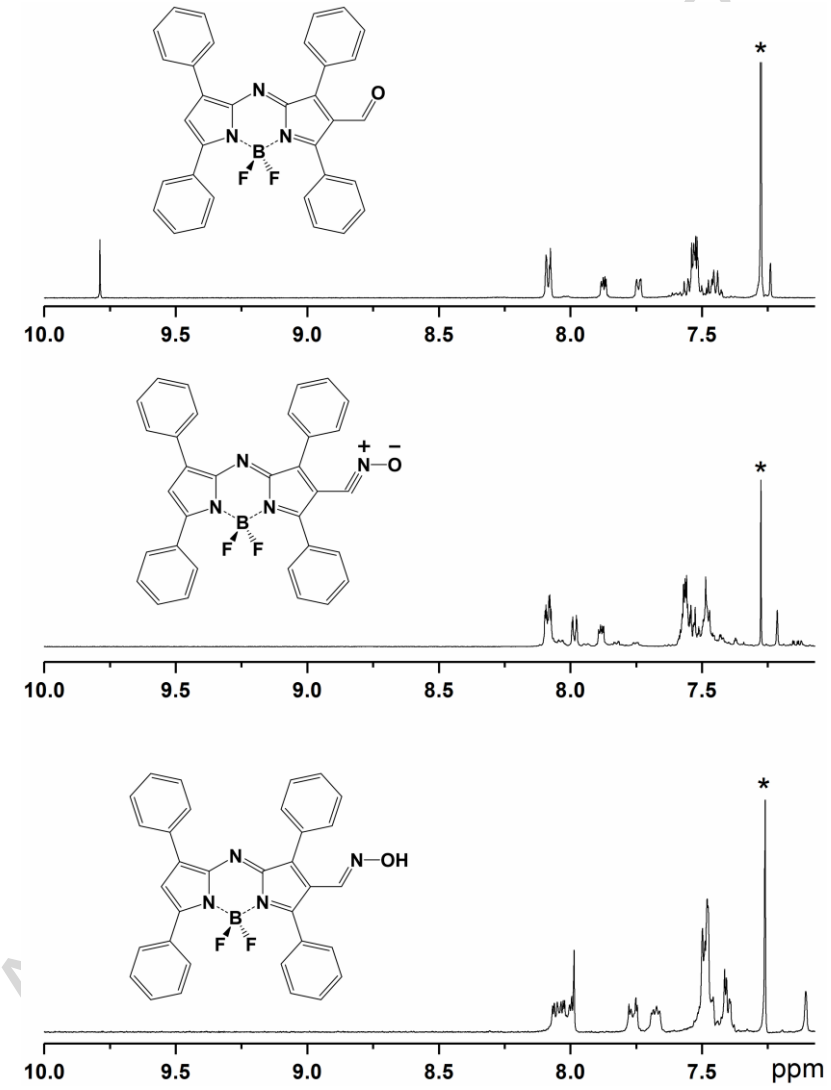

Fig. 5. ^{1}H NMR spectra of the **aza-BODIPY-CNOH** probe and isolated **aza-BODIPY-CNO** in $CDCl_3$-d

Aldoximes as sensing groups for HClO/ClO^- were reported to be transferred to aldehyde[56], nitrile oxide[57], or the carboxylic acid[58]. Here, the aza-BODIPY nitrile oxide product was isolated (**aza-BODIPY-CNO**) when **aza-BODIPY-CNOH** and sodium hypochlorite were mixed. Compared to the

^{1}H NMR spectrum of the **aza-BODIPY-CNOH** probe, the proton on pyrrole of **aza-BODIPY-CNO** was shifted to 7.21 ppm vs 7.11 ppm of that on the probe and the proton peaks of the probe appearing at 7.78-7.66 disappeared accompanying an obvious new peak at 7.98 ppm. The MALI-TOF-MS demonstrated the molecular ion peak of **aza-BODIPY-CNO** at m/z 538.1777 (calculated at 538.1788) (Fig. S6). Based on the characterization of the isolated product including NMR and HRMS, the turn-on fluorescence of the probe **aza-BODIPY-CNOH** in the presence of HClO might come from the oxidation degradation of the aldoxime group of the aza-BODIPY core [57]. Here, the aldoxime group may be converted into the nitrile oxide and hence the rotation and isomerization effects of the aldoxime group are removed. Additionally, the rigid nitrile C≡N may slightly extend the π conjugation of aza-BODIPY core and therefore the LUMO-HOMO energy gap agrees with the small red-shift in absorption and emission wavelengths showed in Figs. 1-2.

2.6 Cell imaging

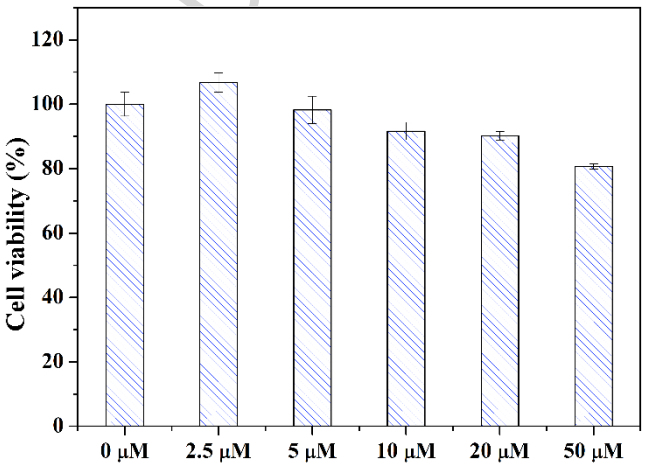

Fig. 6. Cell viability of the RAW264.7 cells in the presence of the **aza-BODIPY-CNOH** probe.

To demonstrate the potential application in biological fields, the MTT and cell imaging experiments were explored and the results were shown in Figs. 6-7. As shown in Fig. 6, even high concentration (50 μM) of the **aza-BODIPY-CNOH** probe was used, the cell variability was still above 80%, showing its low toxicity

and good biocompatibility to living cells. Therefore, the probe has potential application in vivo experiments. Next, the confocal fluorescence imaging experiments were conducted in living RAW264.7 cells (Fig. 7). The probe demonstrated the good permeability and stained in cells with the very weak red-fluorescence as shown in Fig. 7, a-c. Addition of 10 μM of sodium hypochlorite solution to the living cells pre-treated with the probe for 10 min followed by wash thrice using PBS buffer caused the bright red fluorescence emission from living RAW264.7 cells (Fig. 7, e and f). When the living cells were treated with 10 μM of the probe for 10 min and then 25 ng/mL of phorbol ester 12-myristate 13-acetate (PMA) was introduced and incubated for 2 h, PMA also induced the bright red fluorescence (Figs. 7, h and i). All the bright field and emerged images confirmed the intracellular red emission. The results above indicated the **aza-BODIPY-CNOH** probe has good sensing ability for exogenous and endogenous HClO in living cells.

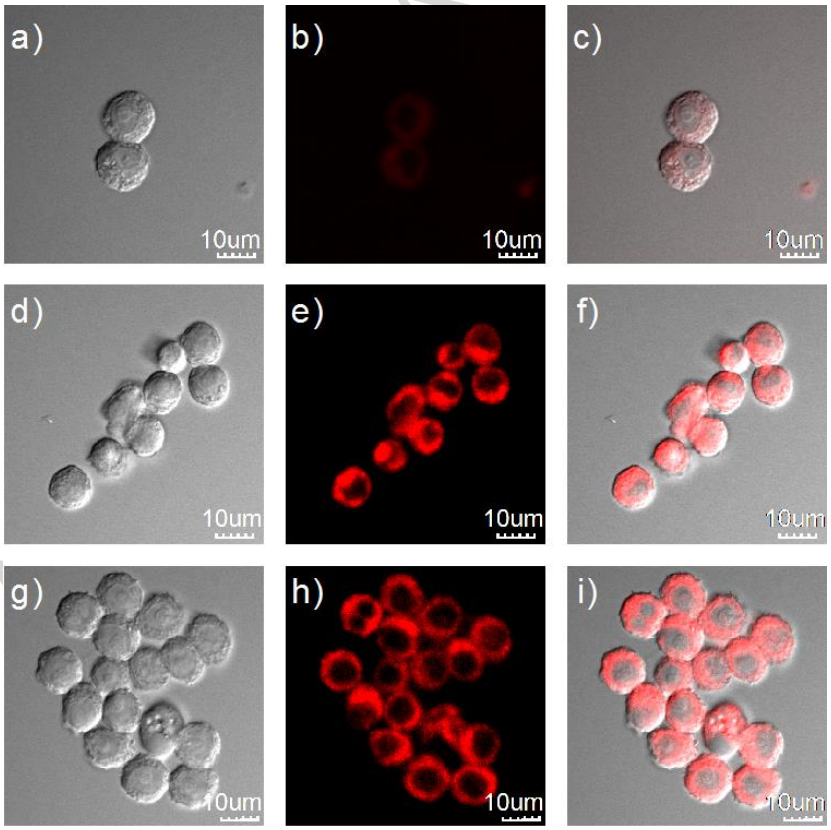

Fig. 7. Fluorescence images of the RAW 264.7 cells incubated with 10 μM of **aza-BODIPY-CNOH** probe for 30 min (top) and 10 μM of **aza-BODIPY-CNOH** probe (10 min) followed by treatment of sodium hypochlorite (10 μM) for 1h (middle) or PMA

(25 ng/mL) (bottom) for 2 h for exogenous and endogenous HClO imaging, respectively. a, d, g: bright field images; b, e, h: fluorescence images ; c, f, i: emerged images of bright field and fluorescence images.

3. Conclusions

An aldoxime-based probe with an aza-BODIPY core has been synthesized and characterized using NMR, IR, and HRMS spectra. The **aza-BODIPY-CNOH** probe can selectively detect HClO based on the turn-on red fluorescence. Other ions including H_2O_2, NO, NO_2^-, NO_3^-, O_2^-, $^1O_2$, ·OH, $ONOO^-$, t-BuOOH, F^-, Cl^-, Br^-, I^-, HCO_3^-, CO_3^{2-}, HSO_4^{2-}, $H_2PO_4^-$, ClO_4^-, S^{2-}, SO_3^{2-}, SO_4^{2-}, Al^{3+}, Ca^{2+}, Zn^{2+}, Pb^{2+}, Cr^{3+}, Fe^{3+}, Cu^{2+}, Hg^{2+}, K^+, Mn^{2+}, Mg^{2+}, Na^+, Ni^+ and Ag^+ did not significantly affect the sensing of the probe to HClO. The oxidation product isolated from the reaction of the probe and sodium hypochlorite were characterized, indicating the aldoxime group of the probe **aza-BODIPY-CNOH** was oxidized to the nitrile oxide to form a new **aza-BODIPY-CNO** compound which was responsible for the development of the turn-on red fluorescence. The **aza-BODIPY-CNOH** probe can penetrate and stain in living cells. The probe inside living RAW264.7 cells showed good response to exogenous and endogenous HClO by adding sodium hypochlorite and PMA induction. The survival rate experiments reflected low toxicity of the probe to living cells, suggesting the potential in vivo experiments.

4. Experimental section

4.1 Materials and instruments

The cell line used was purchased from American Type Culture Collection (ATCC, USA). PMA and other chemicals including organic solvents were obtained from Sigma-Aldrich and TCI. NMR, IR and high-resolution mass spectra were recorded using the Bruker AVANCE III spectrometers, the Thermo Fisher Nicolet 6700 and the DECAX-60000 mass spectrometer, respectively. Fluorescence and absorption spectra were obtained using the Hitachi F-7000 fluorescence spectrometer and the GE Healthcare Ultraspec 3300

spectrophotometer. An FV1000 confocal fluorescence microscope was used to collect the images of the living cells.

4.2 Synthesis of the probe aza-BODIPY-CNOH

To a three-neck-round flask, aldehyde aza-BODIPY[59] (100 mg, 0.19 mmol) and 10 mL pyridine were added and then the mixture was heated at 60 °C with agitation. Next, hydroxylamine sulfate (65 mg, 0.76 mmol) was added at multiple times and the reaction was monitored using TLC. After 8 h, the mixture was evaporated and the solid was dissolved in dichloromethane, followed by filtration. The filtrate was concentrated and the product was purified using the silica gel column chromatography (dichloromethane: n-hexane = 10:1) to obtain 24 mg of the **aza-BODIPY-CNOH** probe. Yield: 21.6%. ^{1}H NMR (500 MHz, $CDCl_3$, ppm) δ 8.07-7.99 (m, 5H), 7.78-7.77 (m, 2H), 7.69-7.66 (m, 2H), 7.5-7.39 (m, 12H), 7.11 (s, 1H). ^{13}C NMR (125 MHz, $CDCl_3$, ppm) δ 144.34, 131.87, 131.70, 131.64, 131.60, 131.01, 130.67, 130.33, 130.22, 130.17, 130.01, 129.96, 129.91, 129.52, 129.26, 128.89, 128.84, 128.11, 127.98, ESI-MS calculated for $[M+H]^+$ at 541.2 and $[M+Na]^+$ at 563.2; HRMS calculated for $[M-H]^-$ at 539.1866, found: 539.1927.

4.3 General procedures for the fluorescence and UV-vis spectra measurement

The stock solution of the **aza-BODIPY-CNOH** probe (1.0 mM) was prepared in acetonitrile. The test solutions were set up at 10 μM (HEPES-acetonitrile, v/v = 1:1, pH = 7.2). The competitive cations and aions used in stock solutions (10 mM) are Al^{3+}, Ca^{2+}, Zn^{2+}, Pb^{2+}, Cr^{3+}, Fe^{3+}, Cu^{2+}, Hg^{2+}, K^+, Mn^{2+}, Mg^{2+}, Na^+, Ni^+, Ag^+, F^-, Cl^-, Br^-, I^-, HCO_3^-, CO_3^{2-}, HSO_4^{2-}, $H_2PO_4^-$, ClO_4^-, S^{2-}, SO_3^{2-}, SO_4^{2-}, NO_2^- and NO_3^-. ROS and RNS including HClO, H_2O_2, t-BuOOH, •OH, O_2^-, $^1O_2$, $ONOO^-$, NO and O_2^- were obtained from the commercial reagents for HClO, H_2O_2, t-BuOOH and KO_2[60], from Fenton reaction by mixing the same equivalent of H_2O_2 and $FeSO_4{\cdot}7H_2O$ for hydroxyl radical (•OH)[61], by mixing NaOCl and H_2O_2 at a molar ratio of 1:2

for singlet oxygen ($^1O_2$)[62], using sodium nitrite, acidic hydrogen peroxide and sodium hydroxide as reagents for peroxynitrite ($ONOO^-$)[41], and from sodium nitroferricyanide (III) nihydrate for nitric oxide (NO)[63]. Fluorescence measurements were configured at room temperature, 2400 nm per min of the scanning speed, 5 nm and 10 nm slit width for the excitation and emission, respectively.

4.4 Cell imaging

RAW264.7 cells were used in cell imaging, and incubated in the culture dishes until 70-80% space was taken up. 10 μM of the **aza-BODIPY-CNOH** μM (HEPES-acetonitrile, v/v = 1:1, pH = 7.2) was added to the culture dishes and incubated for 30 min at 37 °C and then cells were washed three times with PBS. In order to get exogenous and endogenous HClO fluorescence imaging, 10 μM of sodium hypochlorite (pH = 7.2) and 25 ng/mL of PMA were added individually to the culture dishes where the cells has been pre-treated with the probe for 10 min, and incubated for 1 h and 2 h at 37 ºC, respectively. Each dish above was washed three times with PBS and observed by confocal fluorescence microscope. The cell viability was also performed using MTT colorimetric method. The cells were incubated with varied concentrations of the probe **aza-BODIPY-CNOH** (100 μL) for 24 h at 37 °C and then washed PBS buffer thrice. Next, the cells were incubated with MTT solutions (20 μL, 5 mg/mL) for 4 h at 37 °C. After removing the supernatant and adding 100 μL DMSO, the cell viability was obtained by measuring the absorbance at 490 nm.

Acknowledgements

National Natural Science Foundation of China (21777143 and 81671803) and National Key Research and Development Program (Grant No. 2017YFC0107700) are acknowledged for funding. VN would like to acknowledge support from NSERC and CFI.

References

[1] J.Y. Xie, C.Y. Li, Y.F. Li, Y.J. Fu, S.X. Nie, H.Y. Tan, A near-infrared chemosensor for determination of trivalent aluminum ions in living cells and tissues, Dyes. Pigm. 136(2017) 817-824.

[2] K. Wang, T. Leng, Y. Liu, C. Wang, P. Shi, Y. Shen, W.H. Zhu, A novel near-infrared fluorescent probe with a large stokes shift for the detection and imaging of biothiols, Sens. Actuators B: Chem. 248(2017) 338-45.

[3] T. Myochin, K. Hanaoka, S. Iwaki, T. Ueno, T. Komatsu, T. Terai, T. Nagano, Y. Urano, Development of a series of near-infrared dark quenchers based on Si-rhodamines and their application to fluorescent probes, J. Am. Chem. Soc. 137(2015) 4759-4765.

[4] S. Wang, J. Sun, F. Gao, A turn-on near-infrared fluorescent chemosensor for selective detection of lead ions based on a fluorophore-gold nanoparticle assembly, Analyst. 140(2015) 4001-4006.

[5] J. Barbillat, E.D. Silva, Near infra-red Raman spectroscopy with dispersive instruments and multichannel detection, Spectrochim. Acta. A. 53(1997) 2411-2422.

[6] F.D. Stefani, C. Kohl, Y.S. Avlasevich, N. Horn, A.K. Vogt, A. Klaus Müllen, M. Kreiter, Thermochromic Fluorophores and Their NIR Laser Induced Transformation, Chem. Mater. 18(2010) 6115-6120.

[7] X. Yue, Q. Zhang, Z. Dai, Near-infrared light-activatable polymeric nanoformulations for combined therapy and imaging of cancer, Adv. Drug. Deliver. Rev. 115 (2017) 155–170.

[8] A. Yuan, J. Wu, X. Tang, L. Zhao, F. Xu, Y. Hu, Application of near-infrared dyes for tumor imaging, photothermal, and photodynamic therapies, J. Pharm. Sci. 102(2013) 6-28.

[9] L. Hu, P. Wang, M. Zhao, L. Liu, L. Zhou, B. Li, F.H. Albaqami, A.M. El-Toni, X. Li, Y. Xie, X. Sun, F. Zhang, Near-infrared rechargeable “optical battery” implant for irradiation-free photodynamic therapy, Biomaterials. 163(2018) 154-162.

[10] S.A. Hilderbrand, R. Weissleder, Near-infrared fluorescence: application to in vivo molecular imaging, Curr. Opin. Chem. Biol. 14(2010) 71-79.

[11] A. Haque, M.S.H. Faizi, J.A. Rather, M.S. Khan, Next generation NIR fluorophores for tumor imaging and fluorescence-guided surgery: A review, Bioorg. Med. Chem. 25(2017) 2017-2034.

[12] J.O. Escobedo, O. Rusin, S. Lim, R.M. Strongin, NIR dyes for bioimaging applications, Curr. Opin. Chem. Biol. 14(2010) 64-70.

[13] S. Luo, E. Zhang, Y. Su, T. Cheng, C. Shi, A review of NIR dyes in cancer targeting and imaging, Biomaterials. 32(2011) 7127-7138.

[14] J. Xu, J. Zhai, Y. Xu, J. Zhu, Y. Qin, D. Jiang, A near-infrared fluorescent aza-bodipy probe for dual-wavelength detection of hydrogen peroxide in living cells. Analyst, 141(2016), 2380-2383.

[15] W. Zhao, E.M. Carreira, Conformationally restricted aza-bodipy: a highly fluorescent, stable, near-infrared-absorbing dye, Chemistry. 12(2006) 7254-7263.

[16] N. Balsukuri, S. Mori, I. Gupta, Donor acceptor type ferrocene substituted aza-BODIPYs: Synthesis, optical and electrochemical studies, J. Porphyr. Phthalocya. 20(2016) 719-729.

[17] H. Lu, J. Mack, Y. Yang, Z. Shen, Structural modification strategies for the rational design of red/NIR region BODIPYs, Chem. Soc. Rev. 43(2014) 4778-4823.

[18] X.D. Jiang, J. Zhao, Q. Li, C.L. Sun, J. Guan, G.T. Sun, L.J. Xiao, Synthesis of NIR fluorescent thienyl-containing aza-BODIPY and its application for detection of Hg 2+ : Electron transfer by bonding with Hg 2+, Dyes. Pigm. 125(2016) 136-141.

[19] R. Gresser, H. Hartmann, M. Wrackmeyer, K. Leo, M. Riede, Synthesis of thiophene-substituted aza-BODIPYs and their optical and electrochemical properties, Tetrahedron. 67(2011) 7148-7155.

[20] M. Strobl, T. Rappitsch, S.M. Borisov, T. Mayr, I. Klimant, NIR-emitting aza-BODIPY dyes--new building blocks for broad-range optical pH sensors, Analyst. 140(2015) 7150-7153.

[21] A.M. Durantini, D.A. Heredia, J.E. Durantini, E.N. Durantini, BODIPYs to the rescue: Potential applications in photodynamic inactivation, Eur. J. Med. Chem. 144(2018) 651-661.

[22] M.H.Y. Cheng, R.W. Boyle, Traversing the challenges of extended conjugation: Bacteriochlorins and aza-bodipys, a new era in photomedicine, Photodiagn. Photodyn. 17(2017) A25.

[23] M.R. Momeni, A. Brown, A Local CC2 and TDA-DFT Double Hybrid Study on BODIPY/aza-BODIPY Dimers as Heavy Atom Free Triplet Photosensitizers for Photodynamic Therapy Applications, J. Phys. Chem A. 120(2016) 2550-2560.

[24] S. Awuah, Y. You, Boron dipyrromethene (BODIPY)-based photosensitizers for photodynamic therapy, Rsc Adv. 2(2012)

11169-11183.

[25] Y. Yan, J. Tian, F. Hu, X. Wang, Z. Shen, A near IR photosensitizer based on self-assembled CdSe quantum dot-aza-BODIPY conjugate coated with poly(ethylene glycol) and folic acid for concurrent fluorescence imaging and photodynamic therapy, Rsc Adv. 6(2016) 113991–113996.

[26] L. Huang, J. Zhao, S. Guo, C. Zhang, J. Ma, Bodipy derivatives as organic triplet photosensitizers for aerobic photoorganocatalytic oxidative coupling of amines and photooxidation of dihydroxylnaphthalenes, J. Org .Chem. 78(2013) 5627-5637.

[27] S. Guo, R. Tao, J. Zhao, Photoredox catalytic organic reactions promoted with broadband visible light-absorbing Bodipy-iodo-aza-Bodipy triad photocatalyst, Rsc Adv. 4(2014) 36131-36139.

[28] N. Adarsh, M. Shanmugasundaram, R.R. Avirah, D. Ramaiah, Aza-BODIPY derivatives: enhanced quantum yields of triplet excited states and the generation of singlet oxygen and their role as facile sustainable photooxygenation catalysts, Chemistry. 18(2012) 12655-12662.

[29] T. Mueller, R. Gresser, K. Leo, M. Riede, Organic solar cells based on a novel infrared absorbing aza-bodipy dye, Sol. Energy. Mate.r Sol. Cells. 99(2012) 176-181.

[30] J. Min, T. Ameri, R. Gresser, M. Lorenz-Rothe, D. Baran, A. Troeger, V. Sgobba, K. Leo, M. Riede, D.M. Guldi, Two Similar Near-Infrared Absorbing Benzannulated Aza-BODIPY Dyes As Near IR Sensitizers for Ternary Solar Cells, ACS. App. Mater. Inter. 5(2013) 5609-5616.

[31] T. Li, T. Meyer, R. Meerheim, M. Höppner, C. Körner, K. Vandewal, O. Zeika, K. Leo, Aza-BODIPY dyes with heterocyclic substituents and their derivatives bearing a cyanide co-ligand: NIR donor materials for vacuum-processed solar cells, J. Mater. Chem. A. 5(2017) 10696–10703.

[32] Y. Ge, D.F. O'Shea, Azadipyrromethenes: from traditional dye chemistry to leading edge applications, Chem. Soc. Rev. 45(2016) 3846--3864.

[33] J.M. ZGLICZY, T. STELMASZY, W. Ostrowski, J. Naskalski, J. Sznajd, Myeloperoxidase of Human Leukaemic Leucocytes, FEBS. J. 4(1968) 540-547.

[34] A.J. Kettle, C.C. Winterbourn, Myeloperoxidase: a key regulator of neutrophil oxidant production, Redox.Rep. 3(1997) 3-15.

[35] S.M. Wu, S.V. Pizzo, alpha(2)-Macroglobulin from rheumatoid arthritis synovial fluid: functional analysis defines a role for oxidation in inflammation, Arch. Biochem. Biophys. 391(2001) 119-126.

[36] A. Leichsenring, I. Bäcker, P.G. Furtmüller, C. Obinger, F. Lange, J. Flemmig, Long-Term Effects of (–)-Epigallocatechin Gallate (EGCG) on Pristane-Induced Arthritis (PIA) in Female Dark Agouti Rats, PLoS. ONE. 11(2016) e0152518.

[37] E. Malle, T. Buch, H. Grone, Myeloperoxidase in kidney disease, Kidney. Int. 64(2003) 1956–1967.

[38] W. Zheng, R. Warner, R. Ruggeri, C. Su, C. Cortes, A. Skoura, J. Ward, K. Ahn, A. Kalgutkar, D. Sun, PF-1355, a mechanism-based myeloperoxidase inhibitor, prevents immune complex vasculitis and anti-glomerular basement membrane glomerulonephritis, J. Pharmacol. Exp. Ther. 353(2015) 288-298.

[39] C. Nussbaum, A. Klinke, M. Adam, S. Baldus, M. Sperandio, Myeloperoxidase: a leukocyte-derived protagonist of inflammation and cardiovascular disease, Antioxid. Redox. Signal. 18(2013) 692-713.

[40] G.G. Ceylan, C. Ceylan, B. Gülmemmedov, Ş. Tonyalı, O. Odabaş, A. Gözalan, I. Keleş, Ö. E, Polymorphisms of eNOS, catalase, and myeloperoxidase genes in prostate cancer in Turkish men: preliminary results, Genet. Mol. Res. 15(2016) 15038543.

[41] X. Chen, F. Wang, J.Y. Hyun, T. Wei, J. Qiang, X. Ren, I. Shin, J. Yoon, Recent progress in the development of fluorescent, luminescent and colorimetric probes for detection of reactive oxygen and nitrogen species, Chem. Soc. Rev. 45(2016) 2976-3016.

[42] Y. Chen, T. Wei, Z. Zhang, W. Zhang, J. Lv, T. Chen, B. Chi, F. Wang, X. Chen, A mitochondria-targeted fluorescent probe for ratiometric detection of hypochlorite in living cells, Chin. Chem. Lett. (2017) 1957-1960.

[43] Z. Qu, J. Ding, M. Zhao, P. Li, Development of a selenide-based fluorescent probe for imaging hypochlorous acid in lysosomes, J. Photochem. Photobiol. A. Chem. 299(2015) 1-8.

[44] Q.A. Best, N. Sattenapally, D.J. Dyer, C.N. Scott, M.E. Mccarroll, pH-Dependent Si-Fluorescein Hypochlorous Acid Fluorescent

Probe: Spirocycle Ring-Opening and Excess Hypochlorous Acid-Induced Chlorination, J. Am. Chem. Soc. 135(2013) 13365-13370.
[45] J.J. Hu, N.K. Wong, Q.S. Gu, X.Y. Bai, S. Ye, D. Yang, HKOCl-2 Series of Green BODIPY-Based Fluorescent Probes for Hypochlorous Acid Detection and Imaging in Live Cells, Org. Lett. 16(2014) 3544-3547.
[46] S.K. Lee, M.G. Choi, S.K. Chang, Signaling of chloramine: a fluorescent probe for trichloroisocyanuric acid based on deoximation of a coumarin oxime, Tetrahedron. Lett. 55(2014) 7047-7050.
[47] S.I. Reja, V. Bhalla, A. Sharma, G. Kaur, M. Kumar, A highly selective fluorescent probe for hypochlorite and its endogenous imaging in living cells, Chem. Commun. 50(2014) 11911-11914.
[48] W.L. Wu, Z.M. Zhao, X. Dai, L. Su, B.X. Zhao, A fast-response colorimetric and fluorescent probe for hypochlorite and its real applications in biological imaging, Sens. Actuators B: Chem. 232(2016) 390-395.
[49] W.C. Chen, P. Venkatesan, S.P. Wu, A turn-on fluorescent probe for hypochlorous acid based on HOCl-promoted removal of the C=N bond in BODIPY-hydrazone, New. J. Chem. 39(2015) 6892-6898.
[50] J. Shi, Q. Li, X. Zhang, M. Peng, J. Qin, Z. Li, Simple triphenylamine-based luminophore as a hypochlorite chemosensor, Sens. Actuators B: Chem. 145(2010) 583-587.
[51] S.Y. Yu, C.Y. Hsu, W.C. Chen, L.F. Wei, S.P. Wu, A hypochlorous acid turn-on fluorescent probe based on HOCl-promoted oxime oxidation and its application in cell imaging, Sens. Actuators B: Chem. 196(2014) 203-207.
[52] X.X. Xu, Y. Qian, A novel pyridyl triphenylamine–BODIPY aldoxime: Naked-eye visible and fluorometric chemodosimeter for hypochlorite, Spectrochim. A. Mol. Biomol. Spectrosc. 183(2017) 356-361.
[53] X. Cheng, H. Jia, T. Long, J. Feng, J. Qin, Z. Li, A "turn-on" fluorescent probe for hypochlorous acid: convenient synthesis, good sensing performance, and a new design strategy by the removal of C=N isomerization, Chem. Commun. 47(2011) 11978-11980.
[54] L.C. Adam, I. Fabian, K. Suzuki, G. Gordon, Hypochlorous acid decomposition in the pH 5-8 region, Inorg. Chem. 31(1992) 3534-3541.
[55] R. Pethig, D.B. Kell, The passive electrical properties of biological systems: their significance in physiology, biophysics and biotechnology, Phys. Med. Biol. 32(1987) 933-970.
[56] G. Wu, F. Zeng, S. Wu, A water-soluble and specific BODIPY-based fluorescent probe for hypochlorite detection and cell imaging, Anal. Methods. 5(2013) 5589-5596.
[57] M. Emrullahoğlu, Ü. M, E. Karakuş, A BODIPY aldoxime-based chemodosimeter for highly selective and rapid detection of hypochlorous acid, Chem. Commun. 49(2013) 7836-7838.
[58] G. Cheng, J. Fan, W. Sun, K. Sui, X. Jin, J. Wang, X. Peng, A highly specific BODIPY-based probe localized in mitochondria for HClO imaging, Analyst. 138(2013) 6091-6096.
[59] S. Kumar, H.B. Gobeze, T. Chatterjee, F. D'Souza, M. Ravikanth, Directly Connected AzaBODIPY-BODIPY Dyad: Synthesis, Crystal Structure, and Ground- and Excited-State Interactions, J. Phys. Chem. A. 119(2015) 8338-8348.
[60] A.E. Albers, V.S. Okreglak, C.J. Chang, A FRET-based approach to ratiometric fluorescence detection of hydrogen peroxide, J. Am. Chem. Soc. 128(2006) 9640-9641.
[61] X. Li, G. Zhang, H. Ma, D. Zhang, A. Jun Li, D. Zhu, 4,5-Dimethylthio-4‘-[2-(9-anthryloxy)ethylthio]tetrathiafulvalene, a Highly Selective and Sensitive Chemiluminescence Probe for Singlet Oxygen, J. Am. Chem. Soc. 126(2004) 11543-11548.
[62] S. Maity, S. Das, C.M. Sadlowski, J. Zhang, G.K. Vegesna, N. Murthy, Thiophene bridged hydrocyanine - a new fluorogenic ROS probe, Chem. Commun. 53(2017) 10184-10187.
[63] G. Chen, F. Song, J. Wang, Z. Yang, S. Sun, J. Fan, X. Qiang, X. Wang, B. Dou, X. Peng, FRET spectral unmixing: a ratiometric fluorescent nanoprobe for hypochlorite, Chem. Commun. 48(2012) 2949-2951.

Graphical abstract

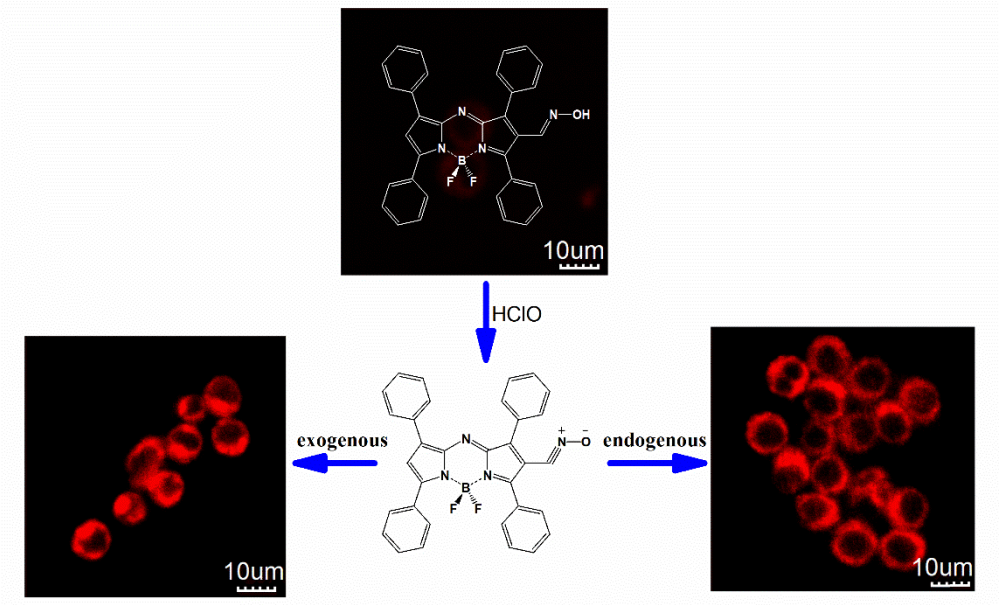

Highlights

- A turn-on aza-BODIPY-CNOH probe has been synthesized and characterized.
- The aza-BODIPY-CNOH probe showed specific fluorescence recognition for HClO.
- The turn-on fluorescence may originate from the aza-BODIPY nitrile oxide product oxidized by HClO.
- The aza-BODIPY-CNOH probe can detect exogenous and endogenous HClO in living cells.